IEEE Access
Multidisciplinary | Rapid Review | Open Access Journal

Date of publication xxxx 00, 0000, date of current version xxxx 00, 0000.

Digital Object Identifier 10.1109/ACCESS.2017.Doi Number

An Integrated Approach Based on Improved CEEMDAN and LSTM Deep Learning Neural Network for Fault Diagnosis of Reciprocating Pump

Fengfeng Bie[1,2], Tengfei Du[3], Fengxia Lyu[1,2], Mingjun Pang[1,2] and Yue Guo[1,2]

[1]School of Mechanical Engineering and Rail Transit, Changzhou University, Changzhou, 213016, China
[2] Jiangsu Key Laboratory of Green Process Equipment, Changzhou University, Changzhou 213164, China
[3] Jiangsu Changjiang Intelligent Manufacturing Research Institute Co., Ltd, Changzhou, 213000, China

Corresponding author: Fengfeng Bie (e-mail: bieff@cczu.edu.cn).

ABSTRACT The reciprocating pump plays an important role in the petrochemical industry procedure, it is crucial in ensuring the systematic safety and stability. Since the useful feature information of the vibration signal from the reciprocating pump tends to be overwhelmed by the background ingredients, it is tough to realize the recognition on typical modes. Aiming at the extraction of reciprocating mechanical fault features and mode recognition, this paper proposes Improved Complete Ensemble Empirical Mode Decomposition with Adaptive Noise and LSTM (Long Short-Term Memory) deep neural network algorithm. Firstly, the IMF components are obtained by decomposing the vibration signals from the reciprocating pump with the Improved CEEMDAN algorithm, in which the key parameter β_k is improved and redefined, for optimizing SNRs (Signal Noise Ratio) of the IMF (Intrinsic Mode Function) components. Then the corresponding singular spectral entropy is calculated and the feature vector is constructed. The classification modal based on LSTM deep network is developed in the data dividing-training and the final mode recognition process. The study shows that the proposed method can effectively extract the fault features of vibration signal of the reciprocating pump, and the testing modes could be accurately recognized with the developed classification model.

INDEX TERMS Improved Complete Ensemble Empirical Mode Decomposition with Adaptive Noise; Long Short-Term Memory; Fault diagnosis; Reciprocating pump; Singular spectrum entropy

I. INTRODUCTION

Reciprocating pump is an important industrial equipment in the field of petroleum, water supply and drainage systems. Due to the complexity of the internal structure and operation mechanism, most of the key parts such as driven and bearing mechanism are vulnerable, which may render huge economic losses in case of system failure [1]. Advancement have been achieved recently in sensor-based real-time monitoring [2], status monitoring, control and optimization [3], key-performance-indicator oriented prognosis and diagnosis for complex industry process systems [4]. As for reciprocating machinery, the fault mechanism analysis, method of feature extraction and typical pattern recognition on transmission parts have always been focused on in relative research field. Unlike the rotary machinery, the impact features from the key reciprocating parts are the main indicator in the typical failure modes, which is regularly overwhelmed in the vibration signal. As the traditional method, vibration-based feature analysis and pattern recognition for state maintenance are focused in related research fields at present. The time-frequency analysis performs effectively applied in extracting fault characteristics from reciprocating pumps vibration signal: EMD (Empirical Mode Decomposition) and improved algorithms such as EEMD (Ensemble Empirical Mode Decomposition) and CEEMDAN (Complementary Ensemble Empirical Mode Decomposition with Adaptive Noise) are developed. In 1998, for the first time, Huang proposed EMD. EMD is a powerful

This article has been accepted for publication in a future issue of this journal, but has not been fully edited. Content may change prior to final publication. Citation information: DOI 10.1109/ACCESS.2021.3056437, IEEE Access

TABLE I
NOMENCLATURE

List of Abbreviations		Symbols	
EEMD	Ensemble Empirical Mode Decomposition	x	The original vibration signal
CEEMDAN	Complementary Ensemble Empirical Mode Decomposition with Adaptive Noise	x^i	The i^{th} constructed signal with white noise
EMD	Empirical Mode Decomposition	W^i	A series of different Gaussian white noise
LSTM	Long Short-Term Memory	$E_k(\,)$	The k^{th} EMD modal component
WPT	Wavelet Packet Transform	r_i	The i^{th} decomposition residual
LTSA	Local Tangent Space Alignment	$\widetilde{d}_i$	The i^{th} modal component
LMD	Local Mean Decomposition	M( )	Local mean of the signal
SVM	Support Vector Machine	β_k	Constant defined in Improved CEEMDAN process
WKNN	weighted *k*-nearest neighbor	ε_k	The k^{th} compensation factor
DT	decision tree	std( )	Standard deviation
DWNN	deep wavelet neural network	μ_i	The singular value of i^{th} IMF component
AE	acoustic emission	S_i	Singular spectral entropy of the signal
IMF	Intrinsic Mode Function	q_i	The proportion of the singular value of the i^{th} IMF
SNR	Signal noise ratio	s	The simulated signal
TP	True positive	s_i	The i^{th} component of the simulated signal
TN	True negative	w	Value of weight
FP	False positive	b	Value of bias
FN	False negative		

tool for dealing with nonlinear vibration signals but EMD decomposition lacks strict mathematical basis, low computational efficiency, and easily causes modal aliasing and false components [5]. On this basis, Liu Z proposed the EEMD algorithm. In the process of EEMD, the modal aliasing can be suppressed to some extent with essential auxiliary white noise added, while the algorithm efficiency is relatively low [6]. For the CEEMDAN algorithm proposed by Torres M E proposed, the adaptive white noise is added to each stage of the decomposition and the modal components by calculating the residuals are obtained, thereby the process improves computational efficiency by reducing modal aliasing [7].

The Improved Complete EEMD with Adaptive Noise method greatly suppresses the modal aliasing problem caused by CEEMDAN's first step decomposition process. In terms of pattern recognition methods, the deep learning method is driven by data and has stronger feature learning ability than traditional machine learning methods. It has significant advantages for analyzing complex and unstructured models [8]. In 2006, Professor Hinton of Canada firstly proposed the idea of deep learning with increasing number of hidden layers and the number of neurons in the neural network, as the improvement, the multi-mode feature classification can be achieved [9].With a wave of deep learning study around the world, it is now widely used in speech recognition, image processing and driverless driving, etc. Introducing deep learning technology into the field of fault diagnosis training and identifying data is a hot trend in fault diagnosis research in the future. The LSTM (Long Short-Term Memory) deep neural network algorithm has stronger learning in the classification process. Recently, data-driven methods have been used for diagnostic research in many devices. A combination of Wavelet Packet Transform (WPT), Local Tangent Space Alignment (LTSA), Empirical Mode Decomposition (EMD) and Local Mean Decomposition (LMD) is studied while the choice of wavelet basis functions is crucial [10]. Reference [11] compares the performance of three classifiers (namely linear Support Vector Machine (SVM), distance-weighted k-nearest neighbor (WKNN), decision tree (DT) using data from optimized and non-optimized sensor set solutions while it's computationally expensive and slow. Reference [12] proposed an improved fault diagnosis method based on a deep wavelet neural network (DWNN), whose practical feasibility was remained to be proven. Reference [13] fused the acoustic emission (AE) signal and the vibration acceleration signal with partly sufficient generalization. Compared with the traditional artificial neural network, the unsupervised deep learning algorithm represented by the AE, is quite different in that deep learning can mine the hidden correlation among the input projects and the compression characteristics of the input data without label intervention. Since the original vibration signal from the reciprocating machinery contains plenty of disturbing noise, it is hard to realize the feature extraction and pattern recognition with traditional single-layer neural network, while the gradient disappearance tends to occur when too many hidden layers involved in the multi-layer neural network, which renders that the iterative process could not converge as required. The critical need exists to evaluate the performance of the deep learning neural network with the typical vibration signal and how best to integrate deep learning with meaningful spectral analysis. Based on this, LSTM method applied in the

research solves the problem of gradient disappearance in the gradient back propagation, with the SNR improved in the preprocessing process, so as to reduce the residual error in the signal decomposition and promote the efficiency of the signal feature extraction.

Aiming at the fault diagnosis method for key parts of reciprocating pump, a fault feature extraction method based on Improved CEEMDAN, singular spectral entropy and LSTM deep neural network algorithm is proposed, in which the dynamic analysis on fault modes of typical reciprocating pump is developed as the primary point, then the diagnosis model is put forward with key parameters calculation and accuracy comparison. Firstly, the Improved CEEMDAN algorithm is used to decompose signal to generate a series of IMF (Intrinsic Modal Function) components. Secondly, the IMF component singular spectral entropy is calculated as the eigenvector. Finally, the feature vector is input into the LSTM deep neural network for training and recognition. Therefore, this paper is organized as follows: Section II is the theoretical foundations of Improved CEEMDAN and LSTM deep learning; Section III illustrates the dynamics simulation and experimental validation, where the proposed method is basically verified on the driven mechanism of the reciprocating pump; the results and discussions on the proposed method are finally presented in Section IV as the ends.

II. PRINCIPLE METHODS

A. IMPROVED CEEMDAN ALGORITHM

By adding positive and negative white noise to each IMF component, the error of IMF reconstruction could be greatly reduced Complete Ensemble Empirical Mode Decomposition with Adaptive Noise (CEEMDAN) is considered as a significant improvement of EEMD. It has been widely used in fields of fault diagnosis, seismology, building energy consumption, etc. Nevertheless, there are several points for further improvements of CEEMDAN: (1) CEEMDAN decomposition of the modal component contains certain residual noise. (2) Since the first step of CEEMDAN decomposition is the same with EEMD method, in the early stage of signal decomposition reconstruction false components are generated while the true signal information characteristics is only involved in the latter IMF components. Reference [14] and [15] pointed out that the components of the original signal and the spurious noise components of the same scale are achieved in the first few components of the decomposition. Aiming at these problems, the Improved CEEMDAN method is proposed. In the first stage of the decomposition, the EEMD algorithm has a local mean and an IMF component, while the true modal component is the average mode of the original signal and noise mixture with some residual noise. On the other hand, the CEEMDAN algorithm employs the residual of the previous modal component decomposition in calculating the next modality with each modal calculation being continuous. Colimenas's Improved CEEMDAN algorithm has better results in signal denoising and decomposition [16]. The Gaussian white noise added in CEEMDAN process is taken instead with a special white noise $E_k(w^{(i)})$ in the Improved CEEMDAN method, which is the k^{th} IMF component from the Gaussian white noise decomposed by EMD, and each modal component calculates the plus noise of the signal. The achieved IMF component is decomposed into the difference between the residual signal and the local mean. The Improved CEEMDAN method greatly reduces the residual noise in the IMF component and remedies the defects of the traditional method that is prone to generate false components and modal aliasing in the early stage of decomposition and reconstruction. The specific decomposition process is as follows:

Step1: Let $x^{(i)} = x + \beta_0 E_1(W^{(i)})$, calculate the first decomposition residual $r_1 = \langle M(x^{(i)}) \rangle$

Step2: Calculate the first modal component when k=1: $\tilde{d}_1 = x - r_1$

Step3: Estimate the second residual as a series of $r_1 + \beta_1 E_2(W^{(i)})$ mean values and define the second modal component: $\tilde{d}_2 = r_1 - r_2 = r_1 - \langle M(r_1 + \beta_1 E_2(w^{(i)})) \rangle$

Step 4: For $k = 3,.....K$ calculating the k^{th} order margin: $r_k = \langle M(r_{k-1} + \beta_{k-1} E_k(w^{(i)})) \rangle$

Step 5: Calculate the K-order mode $\tilde{d}_k = r_{k-1} - r_k$

Step 6: Return to the fourth step to calculate k+1

where $E_k(\,)$ is the k^{th} modal component after EMD decomposition, $M(\,)$ is the local mean of the signal, $w^{(i)}$ be a series of different Gaussian white noise, $<\cdot>$ is the operator which produces the local mean of the signal that is applied to.

Constant defined in Improved CEEMDAN decomposition $\beta_k = \varepsilon_k \frac{std(x)}{std(E_1(w^{(i)}))}$. Since the energy of the signal will gradually decrease during the decomposition process, the equation $E_1(w^{(i)})$ remains unchanged. This cause a problem that in the later stage of signal decomposition, the total energy of the IMF component will decrease after the signal decomposition is extracted, which is one of the reasons for the residual noise. A method for improving parameters β_k is proposed here. Define the parameters $\beta_{ki} = \varepsilon_k \frac{std(x)}{std(E_k(w^{(i)}))}$ so that the white noise energy and the IMF component energy remain the same dimension when mixed with white noise, thus maintaining a stable SNR.

B. SINGULAR SPECTRAL ENTROPY

Information entropy describes the complexity of the information in the signal. The more information contained in the signal, the more complex the signal is [17]. Identically, the more uncertainty and randomness the signal contains, the greater information entropy is. As one of the information entropy, singular spectral entropy reflects the uncertainty of the modes of time domain signals under singular spectrum

partition [18]. The Improved CEEMDAN decomposition of the signal yields an I-order IMF component and a residual r_n.The singular value decomposition is implemented on the IMF components containing different frequency characteristics to obtain the singular value of each IMF component $\mu_1, \mu_2, \mu_3, \ldots \mu_i$. Then the vector $R = [\mu_1, \mu_2, \mu_3, \ldots \mu_i]$ is the singular spectrum of the original signal. The singular spectral entropy of the signal is expressed as:

$$S_1 = -\sum_{i=1}^{M} q_i \log q_i \tag{1}$$

where $q_i = \mu_i / \sum_{i=1}^{M} \mu_i$ represents the proportion of the singular value of the i^{th} IMF component in the overall singular value spectrum.

C. LSTM DEEP NEURAL NETWORK MODEL

As shown in Fig.1, the cell of the Long Short-Term Memory [15] neural network is added to process and identify whether the input information in the algorithm is useful. 3 gates are placed in 1 cell set as input gate, output gate and forgetting gate respectively. The LSTM relies on a number of "gates" to allow input features to selectively influence the state of the neural network at each moment. The so-called "gate" structure is a fully connected neural network that uses a sigmoid as an activation function to output a value between 0 and 1. When a feature vector is input to the LSTM neural network for training, it can be judged according to the rules. Only information that complies with the algorithm's certification will be retained, while information that does not match will be refused through the forgotten gate.

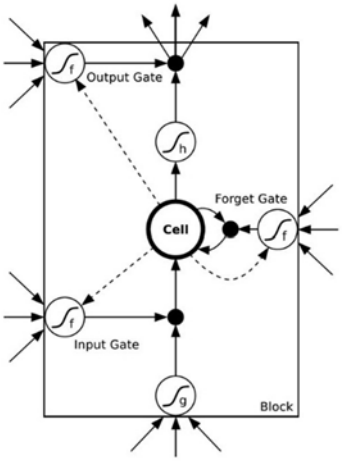

FIGURE 1. LSTM Network Structure

TensorFlow is a general-purpose computing framework developed by Jeff Dean's Google brain team based on Google's first generation of deep learning system, DistBelief [19]. TensorFlow is a system that can design neural networks by itself and transmit complex data structures to the artificial intelligence neural network for analysis and processing [20]. Due to the complexity of the pump structure, the relationship between the various parameters is non-linear. In this paper, an intelligent diagnosis scheme for multi-signal processing technology is proposed. The general flow of the proposed method is shown in the Fig.2.

(1) Collect the original vibration signal of the reciprocating pump, divide the raw data into a training set and testing set.
(2) Process the denoising by the Improved CEEMDAN with improved parameter for stable SNR.
(3) Find sensitive features by singular spectral entropy, and randomly divide the testing and training data for LSTM deep neural network classification.
(4) Construct a new wear diagnosis classifier LSTM, and realize the final classification.

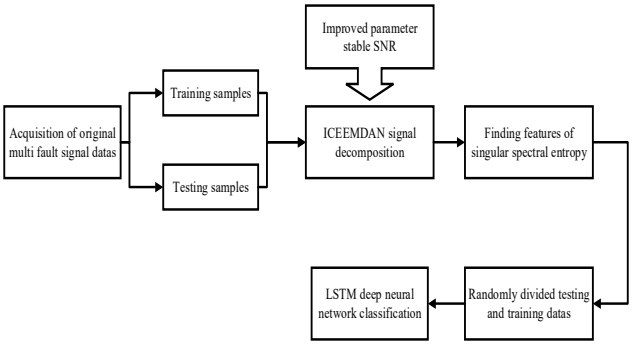

FIGURE 2. Reciprocating pump fault diagnosis flowchart

Based on the TensorFlow framework, a deep neural network system with two hidden layers using Python language is designed, its structure is shown in Fig.3. The data flow diagram generated with TensorBord is shown in Fig.4.

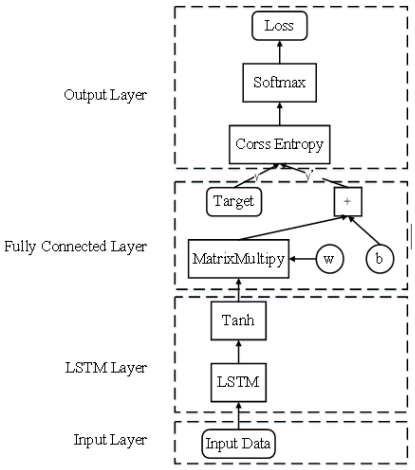

FIGURE 3. Deep LSTM Network Structure

A single training sample feature vector flows from the input layer for the first feature processing through the LSTM neural network, then enters the full connect layer for the second feature processing and finally the loss function is calculated. The *tanh* function is selected as LSTM layer activation function and the *softmax* function is the full-connect activation, then the average value of all the training sample loss functions in each epoch is calculated. As the result, the cost function is calculated and the global minimum of the cost function is achieved with gradient descent.

This article has been accepted for publication in a future issue of this journal, but has not been fully edited. Content may change prior to final publication. Citation information: DOI 10.1109/ACCESS.2021.3056437, IEEE Access

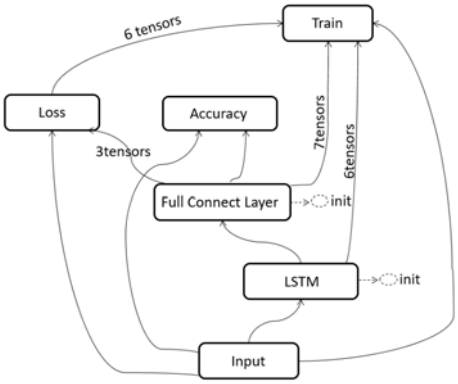

FIGURE 4. **TensorFlow data flow diagram**

III. SIMULATION AND EXPERIMENTAL

A. SIGNAL SINMULATION

Apparently, characteristics of periodical impact shock could be found in the vibration signal of reciprocating pump [21]. In order to verify the effectiveness of the Improved CEEMDAN decomposition for the reciprocating impact signal, the analog signal s is constructed with four components with various parameters (frequency and phase) for the decomposition comparison of Improved CEEMDAN decomposition the CEEMDAN method.

$$s_1 = 12\sin(70\pi t - 2\pi/5)$$
$$s_2 = 7\sin(26\pi t - 3\pi/5)$$
$$s_3 = 4\sin(10\pi t - 4\pi/5)$$
$$s = s_1 + s_2 + s_3 + s_4 \quad (2)$$

where s_4 is a noise signal with amplitude of 0.2. The time domain diagram of the simulated signal components are shown in Fig.5.

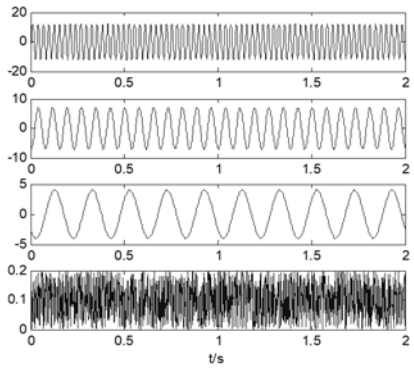

FIGURE 5. **Time domain components of the simulation signal**

The methods of CEEMDAN decomposition and Improved CEEMDAN decomposition are implemented upon the simulation signals respectively, and the results are shown in Fig. 6. The frequency domain diagram of CEEMDAN and Improved CCEMDAN decomposition of each IMF component is shown in Fig. 7, from which the performance on modal aliasing of the two methods are analyzed.

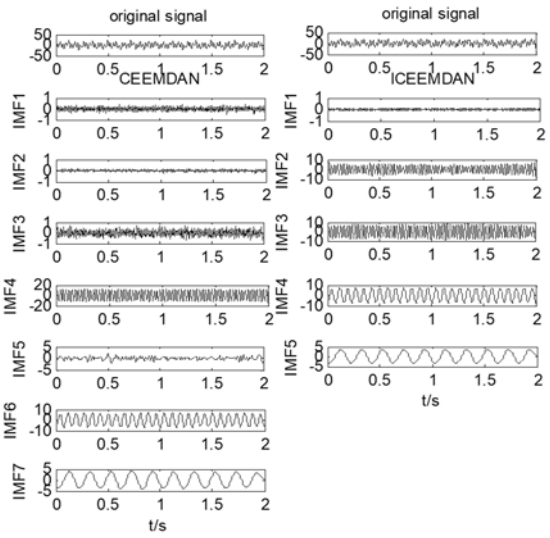

FIGURE 6. **Simulation signals decomposed with original CEEMDAN (left) and** Improved CEEMDAN(**right**)

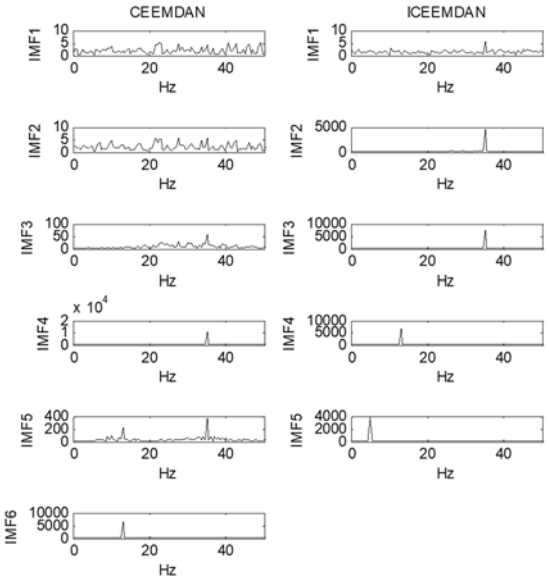

FIGURE 7. **CEEMDAN and Improved CEEMDAN decomposition IMF component of the frequency domain**

Totally 12 IMF components from CEEMDAN are obtained, the first 7 of which are shown in Fig.6, while the Improved CEEMDAN generates 5 IMF components. It can be found from the frequency domain figure of CEEMDAN decomposition in Fig.7 that the first 3 could be classified as false components with no actual physical meaning, while the frequency scale of IMF5 spans two sinusoidal signal frequencies which may render modal aliasing.

Therefore, the Improved CEEMDAN decomposition generates fewer IMFs. From the frequency domain figure, the IMF1 of the Improved CEEMDAN decomposition is the mixed noise component s4. The IMF2 and IMF3 could be expressed as the components s1 that make up the original signal. The ingredient of IMF4 reflects the component s2 that makes up the original signal, while the IMF5 is the

component s3. Each IMF component contains a unique frequency with no modal aliasing, which indicates that the Improved CEEMDAN decomposition has a superior performance.

B. DYNAMICS SIMULATION

In order to further verify the validity of the method, a crankshaft model is established for ADAMS dynamics simulation, as shown in Fig.8.

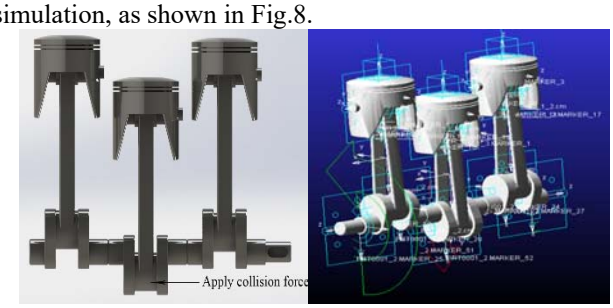

FIGURE 8. Dynamic model of the crankshaft assembly

Normal and fault conditions are simulated in the configuration. As shown in Fig.9，The bearing wear mode is selected as the fault state, in which a collision force on the bearing bush is applied and vibration signal is collected to verify the effectiveness of the proposed method.

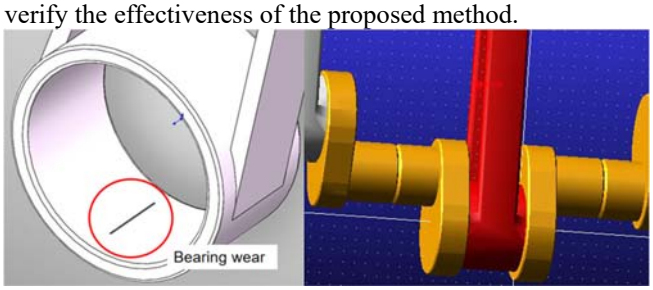

FIGURE 9. Partial drawing of bearing wear

The parameters of the stiffness coefficient, the collision index, the maximum damping coefficient, etc. are involved in the setting of the collision force. The specific parameters are shown in Table II.

TABLE II
CONTACT PARAMETER SETTING

Parameter	Value
Force exponent	1.5
Stiffness coefficient	0.729
Damping coefficient	0.00729
Collision parameters	1.5
Cutting depth	0.1

With the dynamic simulation of targeted configuration, a series of vibration signals from the crankshaft assembly are obtained. The time domains of the typical vibration signals are shown in Fig.10, which illustrates that the periodical impact with different magnitudes of the reciprocating pump is embodied in two typical conditions of normal mode and fault mode. In particular, the impacting features caused by the abnormal force on the bush-crankshaft are added to the simulated fault mode as shown in the time domain signal.

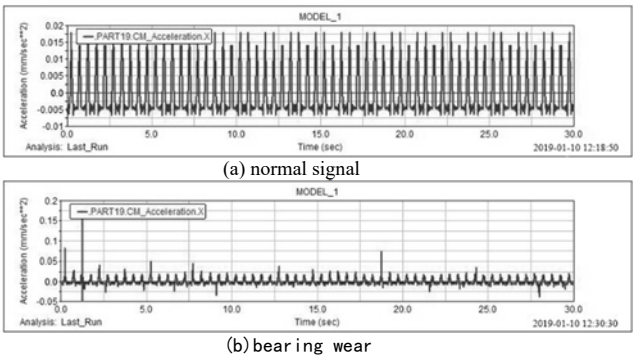

(a) normal signal

(b) bearing wear

FIGURE 10. Normal (up) and fault (down) state acceleration signal

The signal of the bearing pad wear has stronger impact characteristics due to the impact force. For the fault signal, several small peaks could be observed in the frequency band and not as smooth as the normal signal apparently. For quantitative comparisons, further analysis of faults and normal signals is performed to verify the effectiveness of the proposed method. The Improved CEEMDAN decomposition is performed on the analog signal, and the decomposition result is shown in Fig.11.

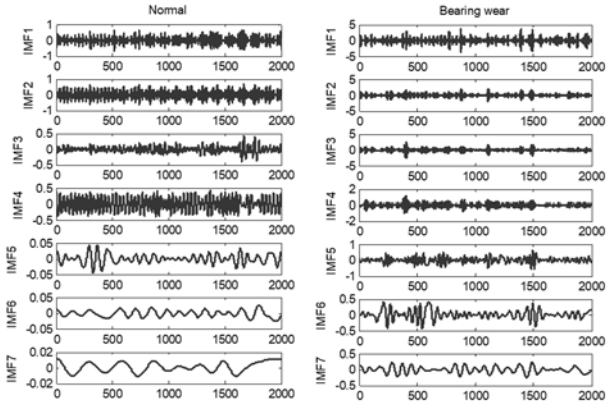

FIGURE 11. Improved CEEMDAN decomposition results left (normal) right (bearing wear)

It can be seen that the magnitude of the normal signal is smaller than that of the fault, indicating that a stronger impact characteristics is involved in the IMF classification of the fault mode. The periodic characteristics of the normal signal are more obviously reflected, and the signal is distorted due to the impact of the fault signal. To quantify the two state characteristics for the analysis，the singular spectral entropy of the normal and bearing wear states is calculated as shown in the Table III.

TABLE III
NORMAL FAULT ENTROPY VALUE

State	Singular spectral entropy
Bearing wear	0.55
Normal	1.42

C. EXPERIMENTAL VALIDATION

Aiming at the vibration measurement on the reciprocating machinery of different running mode, a corresponding testing system is composed, which contains an IEPE

piezoelectric accelerometer with a sensitivity of 102mv/g, a dynamic signal analyzer (type of DH5981) with a mobile power supply and a laptop, as shown in Fig.12. The reciprocating pump experiment platform is shown in Fig.13, which executes a variety of typical failure modes of piston wear, bearing wear, valve disc wear and normal operation. In view of avoiding the signal contamination in the transmission process, the measuring location is set near the driven mechanism of the pump power end, as shown in Fig.14.

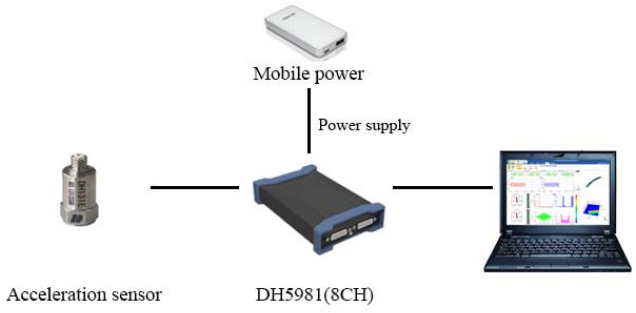

FIGURE 12. **Testing system composition**

FIGURE 13. **Reciprocating pump experiment platform**

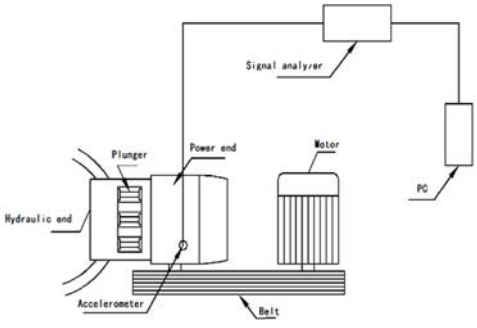

FIGURE 14. **Measuring location arrangement**

D. DATA PROCESSING ANALYSIS AND FEATURE EXTRACTION

The vibration signal of the reciprocating pump under the four conditions of piston wear, bearing wear, valve disc wear and normal operation were collected. The methods of Improved CEEMDAN and CEEMDAN for vibration signal of the four modes are performed individually, and the singular spectral entropy is calculated with the IMFs analyzed and compared. Due to space limitations, only mode of bearing wear is illustrated in Fig.15. It can be observed from the figure that the IMF1 component of (a) and (b) contains similar waveform, while the IMF2 of (a) and the IMF3 of (b) are roughly similar, the IMF3 (a) is similar with The IMF4 (b), meanwhile the magnitude of IMF2 t of the CEEMDAN decomposition is much smaller with the signal waveform varying smoothly.

As mentioned in reference [13], the components of the original signal and the spurious noise components of the same scale tends to generate in the first few components of CEEMDAN process, therefore it could be inferred that the IMF2 in (b) is a spurious component. By comparing and analyzing the IMF3 component in the graph (a) and the IMF4 component in the graph (b), it can be found that the IMF4 contains extra noise information, which may result in information distortion for the possible modal overlap and aliasing phenomenon in the decomposition process. As the overall comparison, Improved CEEMDAN method performs better than CEEMDAN in the feature extraction process.

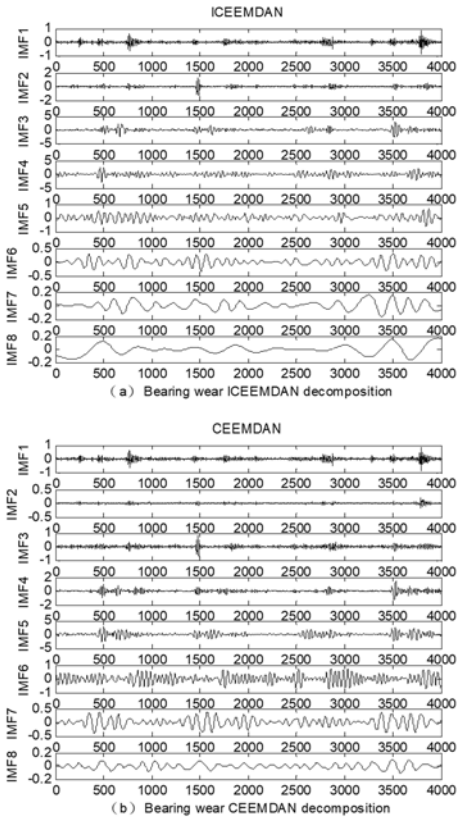

FIGURE 15. **Improved CEEMDAN and CEEMDAN Decomposition on Bearing wear mode**

The effects of the original parameters β_k and the optimized parameters β_{ki} on the SNR of the IMF components are compared and analyzed. The results are shown in Table IV. It could be found that the SNR ratio of the latter IMF

components decreases continuously as the IMF component increases with the parameters before optimization, which means the proportion of the added white noise increases. With the residual noise reducing to some extent, each of the IMF components with improved parameters maintains a relatively stable SNR.

The theory of information entropy shows that singular spectral entropy could reflect the uncertainty and complexity of signal energy distribution. With the singular values of the individual IMF components calculated, the singular spectral entropy values of the signals are obtained according to the singular spectral entropy theory which is shown in Table V. It can be found from Tab.3 that the singular spectral entropy value in fault modes are smaller than the normal. Among the four, the Fault 1 has the smallest singular spectral entropy value since stronger impact characteristics involved in.

TABLE IV
SINGULAR SPECTRUM ENTROPY VALUE OF 4 FAILURE MODES

Fault type	Fault 1	Fault 2	Fault 3	Normal
Singular spectral entropy	0.4995	1.2058	1.0119	1.3768

D. PATTERN RECOGNITION ON LSTM MODEL

In this paper, totally 2000 sets of samples of Fault 1, Fault 2, Fault 3 and Normal signals (500 groups each) are extracted from the original vibration data. Each set of data samples contains 2048 points, and the 500 sets of data for each category were divided into two categories, 400 of which were used for training and 100 for testing. As the result, 1600 sets of samples for training and 400 sets of samples for testing are obtained.

TABLE V
PROGRAMMING PARAMETERS

Parameter name	parameter value
Batch	50
Epoch	500
LSTM layer activation	Tanh
Full connection layer activation function	Softmax
Loss function	Cross Entropy
Training method	Gradient Descent
Learning rate	0.2

Since the final output layer is selected by the softmax activation function, the four sample labels are in one-hot mode for training and testing, and the bearing wear is defined as [1,0,0,0]; the piston wear is [0,1, 0,0]; disc wear is [0,0,1,0]; normal is [0,0,0,1]. The entire neural network was composed of an input layer (Input); a hidden layer (LSTM layer, Full Connect Layer) and an output layer (Loss). The data flows in from the input layer, passes through the LSTM neural network and no linearize through the *tanh* activation function, then the fully connected layer functioned with the softmax function, finally the output was achieved. The related specific parameters are shown in Table VI.

TABLE VI
PARAMETER OPTIMIZATION SNR COMPARISON

Parameter	SNR Unit (dB)									
β_{ki}	IMF_1	IMF_2	IMF_3	IMF_4	IMF_5	IMF_6	IMF_7	IMF_8	IMF_9	IMF_{10}
	30.24	29.34	30.79	32.50	33.96	33.61	34.32	32.56	27.90	30.78
β_k	IMF_1	IMF_2	IMF_3	IMF_4	IMF_5	IMF_6	IMF_7	IMF_8	IMF_9	IMF_{10}
	34.99	29.41	28.12	31.15	34.04	28.84	24.44	14.93	14.40	10.38

The LSTM deep neural network loss function size after 500 iterations as shown in Fig.16. The accuracy after 500 training sessions is shown in Fig.17. The loss function decreases rapidly in the first 100 epochs, then the convergence tends to be stable and the loss function converges. The accuracy of classification is continuously improved with the training, it rises up to 95% after 500 trainings.

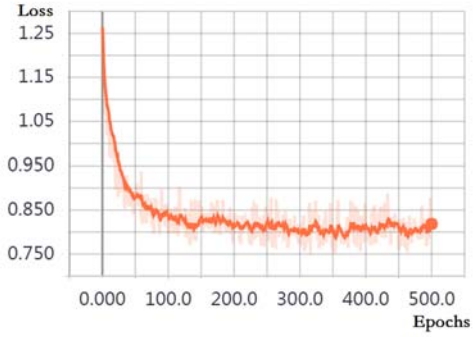

FIGURE 16. Size of the Loss Function

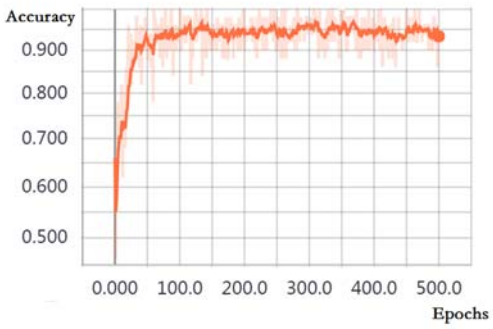

FIGURE 17. Training accuracy

The original sampling data is labelled according to the fault type, among which 40% is selected as training set, 50% as testing set and the residual 10% for the final modal verification. With the fault value labelled as *positive* and normal as *negative*, the accuracy is calculated here for the comparison:

This article has been accepted for publication in a future issue of this journal, but has not been fully edited. Content may change prior to final publication. Citation information: DOI 10.1109/ACCESS.2021.3056437, IEEE Access

$$Accuracy=\frac{TP+TN}{TP+FN+FP+FN} \quad (3)$$

With the same configuration, the feature data is respectively input into the traditional classifiers such as PNN neural network, RBF neural network and BP neural network. As shown in Fig.18, the recognition accuracy of LSTM deep, PNN, RBF and BP neural network under one batch (50 test samples) is compared. The recognition accuracy of LSTM deep neural network testing set is 95% and PNN neural network is only 90%. Table VII shows a comparison of the recognition accuracy of various neural network algorithms.

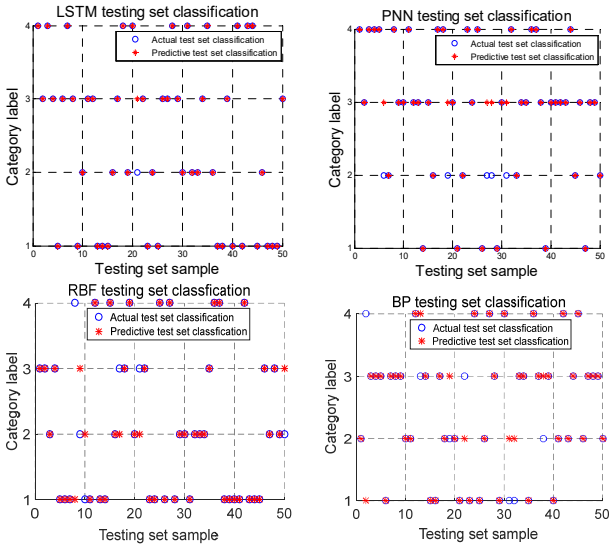

FIGURE 18. LSTM, PNN, RBF and BP Neural Network Identification

TABLE VII
COMPARISON OF RECOGNITION ALGORITHM PREDICTION RESULTS

Classification	LSTM	PNN	RBF	BP
Training sample accuracy (%)	96	92	90	90
Testing sample accuracy (%)	95	90	88	85

IV. CONCLUSIONS

An improved simulation and analysis method based on the CEEMDAN and LSTM has been proposed in order to accurately extract the typical characteristics and identify the fault patterns of the reciprocating pump. The method is based on acceleration data recorded on the vibrating case of reciprocating machinery. The decomposition results of Improved CEEMDAN and traditional CEEMDAN decomposition in signal processing are compared and analyzed on the vibration signal of the normal and typical fault modes of the reciprocating pump, the singular spectral entropy feature vector is constructed afterwards, then the feature vector is input into the LSTM deep neural network for the final pattern recognition. The specific conclusions are as follows:

(1) Through simulation and experimental analysis, it is testified that Improved CEEMDAN decomposition performs better on complex vibration signals of reciprocating machinery in averting false components and modal aliasing as in the traditional CEEMDAN method.

(2) The signal processing method based on Improved CEEMDAN and singular spectral entropy is proposed. The experimental results show that the features of the reciprocating pump could effectively extracted through the method.

(3) Comparative analysis of LSTM deep neural network and other classical machine learning neural networks (RBF, PNN, BP) is implemented for the final pattern recognition. LSTM neural network based on deep learning has a more accurate recognition rate as the research result.

ACKNOWLEDGMENT

The authors gratefully acknowledge the support of the National Natural Science Foundation of China (No.51376026) and Major Project of Natural Science Research in Universities of Jiangsu province (No.19KJA430004).

REFERENCES

[1] Y.B. Jing, C. W. Liu, F.R. Bi, et al. “Diesel Engine Valve Clearance Fault Diagnosis Based on Features Extraction Techniques and FastICA-SVM,” *Chinese Journal of Mechanical Engineering*, vol.30, pp.1-17, Aug. 2017.

[2] S. Yin, R. Andina J J, Y. Jiang. Real-Time Monitoring and Control of Industrial Cyberphysical Systems: With Integrated Plant-Wide Monitoring and Control Framework. *IEEE Industrial Electronics Magazine*, 2019, vol.13. pp.38-47, Dec. 2019.

[3] Y. Jiang, S. Yin, J. Dong, et al. A Review on Soft Sensors for Monitoring, Control and Optimization of Industrial Processes, *IEEE Sensors Journal*, vol.1, Oct. 2020. doi: 10.1109/JSEN.2020.3033153.

[4] Y. Jiang, S. Yin. Recent advances in key-performance-indicator oriented prognosis and diagnosis with a matlab toolbox: dbkit. *IEEE Transactions on Industrial Infomatics*, vol.15, pp. 2849–58, May. 2019.

[5] J. Wang, Guifu. Du, Z. Zhu, et al. “Fault diagnosis of rotating machines based on the EMD manifold,” *Mechanical Systems and Signal Processing*, vol.135, pp.1-21, Jan. 2020.

[6] Z. Liu, W. Sun, J. Zeng. “A new short-term load forecasting method of power system based on EEMD and SS-PSO,” *Neural Computing & Applications*, vol.24, pp. 973-983, Mar. 2014.

[7] M. E. Torres, M. A. Colominas, G. Schlotthauer, et al. “A complete ensemble empirical mode decomposition with adaptive noise,” in *Proc. IEEE International Conference on Acoustics, Speech and Signal Processing*., Prague , Czech, 2011, pp.4144-4147.

[8] O. Janssens, R. V. Walle, M. Loccufier, et al. “Deep Learning for Infrared Thermal Image Based Machine Health Monitoring,” *IEEE/ASME Transactions on Mechatronics*, vol.23, pp. 151-159, Dec. 2018.

[9] B. T. Pham, D. T. Bui, I. Prakash, et al. “Hybrid integration of Multilayer Perceptron Neural Networks and machine learning ensembles for landslide susceptibility assessment at Himalayan area (India) using GIS,” *Catena*, vol.149, pp.52-63, 2017.

[10] Y. Lan, J. Hu, J. Huang, et al. Fault Diagnosis on Slipper Abrasion of Axial Piston Pump based on Extreme Learning Machine, *Measurement*, vol.124, pp.378-385, Aug.2018.

[11] M. Jung, O. Niculita, Z. Skaf. “Comparison of Different Classification Algorithms for Fault Detection and Fault

Isolation in Complex Systems," *Procedia Manufacturing*, vol.19, pp.111-118, 2018.

[12] Z. Zhang , Q. Yun , Dou A . "An improved K-means algorithm for reciprocating compressor fault diagnosis," in *Proc.CCDC*, Shenyang, China, 2018, pp.276-281.

[13] S. Deng, J. Pei , Y. Wang, et al. "Research on drilling mud pump fault diagnosis based on fusion of acoustic emission and vibration technology," *Insight - Non-Destructive Testing and Condition Monitoring*, vol.59, pp. 415-423, Oct. 2017.

[14] Y. Zhang, J. Ji, B. Ma. "Fault diagnosis of reciprocating compressor using a novel ensembleempirical mode decomposition-convolutional deep belief network," *Measurement*, vol.156, pp.1-12, Jun. 2020.

[15] W. Huang. J. Zeng, Z. Yang, et al. "Partial noise assisted multivariate EMD: An improved noise assisted method for multivariate signals decomposition," *Biomedical Signal Processing and Control*, vol.36, pp.205-220, Jul 2017.

[16] M. A. Colominas, Schlotthauer G, Torres M E. "Improved complete ensemble EMD: A suitable tool for biomedical signal processing," *Biomedical Signal Processing & Control*, vol.14, pp.19-29, Jan. 2014.

[17] X. Zhang, C. Mei, D. Chen, et al. "Feature selection in mixed data: A method using a novel fuzzy rough set-based information entropy," *Pattern Recognition*, vol.56, pp.1-15, Aug. 2016.

[18] W. Bing, D. Ming, S Kai. "Fault diagnosis of hydrogen sensor based on wavelet singular entropy and relevance vector machine," *Electric Machines & Control*, vol.19, pp.96-101, Oct. 2015.

[19] Bahdanau D, Cho K, Bengio Y. "Improving neural machine translation with sentence alignment learning," *Neurocomputing*, vol.420, pp.15-26, Jan. 2021.

[20] M. Liu, D. Grana. "Accelerating geostatistical seismic inversion using TensorFlow: A heterogeneous distributed deep learning framework." *Computers & Geoscience*. vol. 124, pp. 37-45, Mar. 2019,

[21] J. Pei, H. Chao, M. Lv, et al. "The valve motion characteristics of a reciprocating pump," *Mechanical Systems & Signal Processing*, vol. 66–67, pp. 657-664, Jan. 2016

Fengfeng Bie was born in Xiantao, Hubei, China, 1979. He received the M.S. degree in mechanical engineering from the Northeast Petroleum University in 2004 and Ph.D. degree in mechatronic engineering from Dalian University of Technology, Liaoning Province, in 2008

From 2008 to 2013, he was a lecturer and Research Assistant in Northeast Petroleum University. Since 2013, he has been an Assistant Professor with the School of Mechanical Engineering, Changzhou University. He is the author of two books, more than 50 articles, and holds three patents. His research interests include mechanical fault detection, diagnostics and prognostics, remote monitoring, mechanical intelligent diagnosis systems, and intelligent pattern recognition.

Dr. Bie was a recipient of the Science and Technology Progress Award of China Petroleum and Chemical Industry Association for Excellence in 2019 and Jiangsu Science and Technology award in 2020.

Tengfei Du was born in Changzhou, Jiangsu, China in 1993. He received the M.S. degree in process mechanical engineering from Changzhou University in 2019.

From 2016 to 2019, he was a Research Assistant with Key laboratory of Process Equipment and now he is an engineer in intelligent manufacturing. He was a keynote speaker at the 2018 IWAMA International Conference. His research interests include mechanical equipment reliability testing, mechanical signal processing, intelligent pattern recognition, etc.

Fengxia Lyu was born in Qiqihaer, Heilongjiang, China in 1978. She received the Ph.D. degree in mechanical engineering from Northeast Petroleum University in 2014.

From 2004 to 2014, she was a lecturer and assistant professor in Northeast Petroleum University. Since 2014, she has been an assistant professor with School of Mechanical Engineering, Changzhou University. She is the author of three books, more than 30 articles, and holds two patents. Her research interests include fluid mechanics, mechanical intelligent pattern recognition, mechanism design optimization, etc.

Dr. Lyu was a contributing editor of Journal of Northeast Petroleum University and a recipient of the Science and Technology Progress Award of China Institute of Mechanical Industry Association for Excellence in 2018.

Mingjun Pang was born in Datong, Shanxi, China in 1976. He received the M.S. Degree in Environmental and Chemical Engineering from Nanchang University and the Ph.D. degree in Energy and Power Engineering from Xi'an Jiao tong University in 2011.

Since 2003, he has been a lecturer, assistant professor and professor with School of Mechanical Engineering and Key laboratory of Process Equipment, Changzhou University. He is the author of two books, more than 40 articles, and holds 12 patents. His research fields focus on computational fluid mechanics, fluid dynamics and optimization, pattern recognition.

Yue Guo was born in Shizuishan, Ningxia, China in 1996. Currently, she is studying for a M.S. degree in Power Engineering at School of Mechanical Engineering, Changzhou University and will receive the M.S. degree certificate in 2021.

Since 2018, she has been a Research Assistant with Key laboratory of Process Equipment. She once participated in the Chinese College Students Mechanical Engineering Innovation and Creativity Competition and won the second prize in 2020. She is the author of 4 articles, and holds one invention. Her research interests include mechanical equipment reliability testing, mechanical signal processing, intelligent pattern recognition, etc.